Phytopathology Research

RESEARCH

Open Access

The E2 ubiquitin-conjugating enzyme CfRad6 regulates the autophagy and pathogenicity of *Colletotrichum fructicola* on *Camellia oleifera*

Jing Luo[1,2], Yan Chen[1,2], Yuan Guo[1,2], He Li[1,2] and Shengpei Zhang[1,2*]

Abstract

Anthracnose is a common disease found in *Camellia oleifera* producing areas across China, whose primary pathogen is *Colletotrichum fructicola*. We previously revealed that autophagy is essential for the pathogenicity of *C. fructicola*. However, the function of ubiquitin–proteasome system (UPS), which is a parallel protein degradation pathway to autophagy, remains elusive. Here, we report that CfRad6, an E2 conjugating enzyme in UPS, interacts with three putative E3 ubiquitin ligases, namely CfRad18, CfUbr1, and CfBre1. Importantly, we presented evidence showing that CfRad6 negatively regulates autophagy, revealing the first link between UPS and autophagy in pathogenic fungi. Targeted gene deletion showed that CfRad6 is involved in growth and conidiation. We further found that the Δ*Cfrad6* mutant is defective in appressoria formation and responses to environmental stresses. These combined effects, along with the abnormal autophagy level, lead to the pathogenicity defects of the Δ*Cfrad6* mutant. Taken together, our study indicates the pleiotropic functions of CfRad6 in the development and pathogenicity of *C. fructicola*.

Keywords *Colletotrichum fructicola*, E2 ubiquitin-conjugating enzyme CfRad6, Autophagy, Appressorium, Pathogenicity

Background

Camellia oleifera is a woody plant cultivated for its edible oil plant in the southern provinces of China (Wu et al. 2020). Anthracnose is one of the most important diseases of *C. oleifera* (Li et al. 2016). Our previous research has shown that several species of pathogenic fungi cause anthracnose on *C. oleifera*, with *Colletotrichum fructicola* being the most prevalent and pathogenic (Li et al. 2016; Jiang et al. 2018).

The autophagy and ubiquitin–proteasome system (UPS) are the main cellular quality control systems (Pohl and Dikic 2019). Recently, we revealed that autophagy is essential for the pathogenicity of *C. fructicola* (Guo et al. 2022; Zhang et al. 2022). Autophagy is a common and conserved process in which organelles and proteins are degraded and recycled in vacuoles (lysosomes) (Mizushima and Komatsu 2011; Ohsumi 2014). The UPS is a parallel protein degradation pathway to autophagy in eukaryotic cells (Ciechanover 2005). Furthermore, increasing evidence suggests that the ubiquitination of proteins is not limited to the function of degradation but also participates in many processes, such as intracellular transcription, DNA repair and cell cycle regulation

*Correspondence:
Shengpei Zhang
csufzsp@163.com
[1] College of Forestry, Central South University of Forestry and Technology, Changsha 410004, China
[2] Key Laboratory for Non-Wood Forest Cultivation and Conservation of Ministry of Education, Changsha 410004, China

(Mukhopadhyay and Riezman 2007; Ulrich and Walden 2010). However, the roles of UPS in *C. fructicola* remain elusive, and the relationship between UPS and autophagy in pathogenic fungi is also unknown.

The UPS pathway is composed of several components, including ubiquitin, E1 ubiquitin-activating enzyme, E2 ubiquitin-conjugating enzyme, E3 ubiquitin ligase, 26S proteasome and deubiquitinating enzyme. It is a major non-lysosome (vacuoles) pathway for degrading proteins (Jia et al. 2023). Typically, the ubiquitination process of a target protein involves a three-step sequential transmission reaction of the three ubiquitin enzymes of E1, E2, and E3 (Jentsch et al. 1987). E2 plays a critical role in this process by controlling the conversion of ubiquitin chains from initiation to extension, and determining the mission of the modified target protein by influencing the formation of ubiquitin chain topology (Imura et al. 2015; Stewart et al. 2016).

Previous research revealed that Rad6, an important ubiquitin-conjugating enzyme E2, plays an important role in DNA damage repair by ubiquitinating various target protein (Shukla et al. 2022). In yeast, Rad6 does not function alone but interacts with the other three E3 ubiquitin ligase proteins Bre1, Rad18, and Ubr1 to regulate mono-ubiquitination of histone proteins, DNA replication repair and ubiquitination substrate proteins in cells (Shi et al. 2016). Similarly, Rad6 in rice cells interacts with OsSgt1 to regulate protein degradation and DNA repair (Yamamoto et al. 2004). Moreover, when the soybean *GmUBC2*, the yeast Rad6 homologous gene, was expressed in *Arabidopsis*, it improved the tolerance of *Arabidopsis* cells to osmotic stress (Zhou et al. 2010; Zhang et al. 2018). The studies demonstrate that Rad6 plays a significant role in yeast and plant. Additionally, Rad6-mediated ubiquitination has been found to be crucial in phytopathogens, such as *Magnaporthe oryzae*, where it is required for development and pathogenicity (Shi et al. 2016). In *Fusarium graminearum*, Rad6 mediates the H2B ub1 level and deoxynivalenol (DON) production (Ma et al. 2021). The *Fusarium verticllioides* Ubl1, a homologous of Rad6-mediated E3 Ubr1, is also involved in its pathogenicity on hosts (Ridenour et al. 2014). However, the roles of Rad6 in autophagy and the relationship between UPS with autophagy are unknown in phytopathogens.

In the present study, we analyzed the Rad6-related ubiquitination pathway in *C. fructicola* and characterized its pleiotropic functions. We also provided evidence indicating the links between autophagy and the ubiquitination pathway.

Results

The phylogenetic analysis and the domain prediction of CfRad6

We identified CfRad6 in the database of *C. fructicola* by using the known ScRad6 amino acid sequence from *Saccharomyces cerevisiae*, and a phylogenetic tree of Rad6 proteins was constructed using Neighbor-Joining Algorithm. The result revealed that CfRad6 has the highest homology with *C. gloeosporioides* and is the most distant from the unicellular yeast (Fig. 1a). The CfRad6 protein is composed of 151 amino acids and contains a ubiquitin-coupled catalysis (UBCc) domain that spans amino acids 7 to 150 (Fig. 1b).

Targeted *CfRAD6* gene deletion and complementation

In order to study the biological function of CfRad6 in *C. fructicola*, we utilized homologous recombination to replace the *CfRAD6* coding region with the hygromycin resistance cassette (*HPH*) (Additional file 1: Figure S1a), and the resulting transformants were confirmed by PCR, RT-PCR (Reverse Transcription PCR) and RT-qPCR

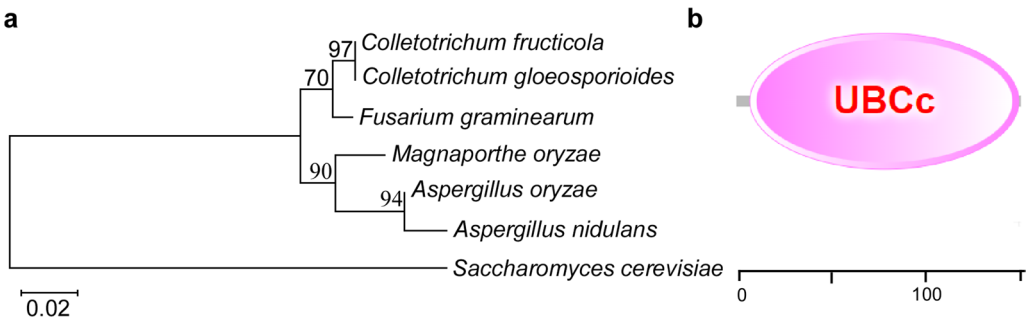

Fig. 1 Phylogenetic analysis of Rad6 protein in fungi and domain prediction of CfRad6. **a** Based on protein sequences of diverse fungi, the phylogenetic tree was constructed by Mega 11.0 program with the Neighbor-joining method. The scale is 0.02. The Latin names of the corresponding species and their NCBI accession numbers are as follows: *C. fructicola* (XP_007273365.1), *C. gloeosporioides* (KAH9242036.1), *F. graminearum* (EYB31908.1), *M. oryzae* (XP_003714754.1), *A. oryzae* (XP_001826971.1), *A. nidulans* (Q96UP5.1), *S. cerevisiae* (AJS07636.1). **b** Domain prediction of CfRad6 by SMART website. The oval (7–150 amino acids) represents the conserved UBCc domain

(Additional file 1: Figure S1b–d). In addition, the wild-type *CfRAD6* gene was re-introduced into the knockout mutant, which restored all defects. We thus obtained the mutant Δ*Cfrad6* and the complemented strain Δ*Cfrad6/CfRAD6*. We first examined the role of CfRad6 in total protein ubiquitination level but found that the ubiquitination level within Δ*Cfrad6* was similar to that of WT and Δ*Cfrad6/CfRAD6* (Additional file 1: Figure S2).

CfRad6 interacts with CfRad18, CfBre1, and CfUbr1 in *C. fructicola*

Rad6 is known to interact with the other three E3 ubiquitin ligase proteins Rad18, Bre1, and Ubr1 (Enserink and Kolodner 2012). In order to elucidate whether there is also an interaction between ubiquitin-conjugating enzyme E2 Rad6 and the three E3 ubiquitin ligases in *C. fructicola*, yeast two-hybrid (Y2H) assays were performed. The results revealed that yeast cells transformed with CfRad6/CfRad18, CfRad6/CfUbr1 and CfRad6/CfBre1 all showed growth on the SD-Leu-Trp-His-Ade medium, indicating that CfRad6 does indeed interact with CfRad18, CfUbr1, and CfBre1 (Fig. 2). This finding suggests that CfRad6 shares the same conserved interaction with E3 ubiquitin ligases in *C. fructicola*.

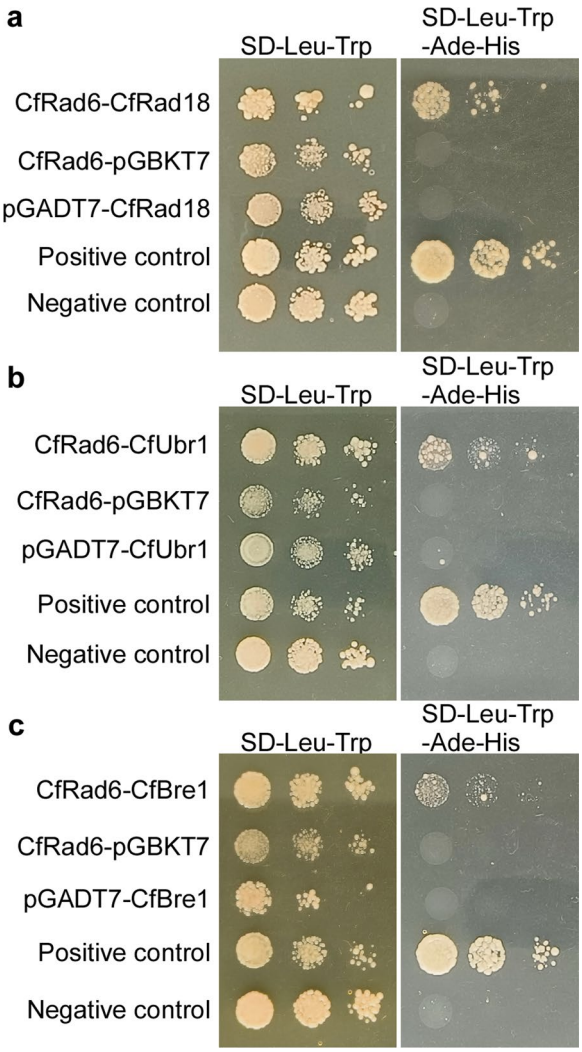

Fig. 2 CfRad6 interacts with CfRad18, CfBre1, and CfUbr1. The pGADT7 and pGBKT7 vectors, fused with the related genes, were co-transformed into the yeast strain AH109. Ten-fold serial dilutions of transformants were spotted in equal volume (5 μL) on synthetic two-deficient media (SD-Leu-Trp) and synthetic quadruple dropout selection media (SD-Leu-Trp-Ade-His). Leu: leucine; Trp: tryptophan: Ade, adenine; His: histidine

CfRad6 is involved in response to rapamycin

To investigate whether there is a link between CfRad6-related UPS and autophagy, we tested the role of CfRad6 in the response to rapamycin, an autophagy inducer that inactivates Tor (the target of rapamycin) pathway (Marroquin-Guzman and Wilson 2015; Wang and Wang 2015). We cultured the wide-type (WT), Δ*Cfrad6* and Δ*Cfrad6/CfRAD6* strains on PDA medium supplemented with 25 nM rapamycin. The results showed that the inhibition rate of Δ*Cfrad6* was significantly lower than that of WT and Δ*Cfrad6/CfRAD6* (Fig. 3). The result indicated that CfRad6 is involved in the response to rapamycin of *C. fructicola*.

CfRad6 negatively regulates the autophagy process

To further investigate the role of CfRad6 in autophagy, the GFP-tagged *CfATG8*, which was used as a marker for autophagy in our previous studies (Guo et al. 2022; Zhang et al. 2022), was transformed into the WT and Δ*Cfrad6* mutant strains. When grown in CM medium, the Δ*Cfrad6* mutant exhibited more autophagosomes than WT. After MM-N induction for 4 h, most of the GFP fluorescence was transferred into the vacuoles, both in WT and Δ*Cfrad6*, but WT still showed some cytoplasmic GFP fluorescence and significantly more autophagosomes than the Δ*Cfrad6* mutant (Fig. 4a,b). We further evaluated autophagic flux by performing GFP-CfAtg8 proteolysis assays through western blotting. In CM condition, WT expressing GFP-*CfATG8* exhibited lower amounts of free GFP than full-length GFP-CfAtg8, but the Δ*Cfrad6* mutant expressing GFP-*CfATG8* exhibited comparable free GFP to GFP-CfAtg8 (Fig. 4c), suggesting the higher autophagy level in the Δ*Cfrad6* mutant under rich nutrients. When induced in MM-N for 4 h, WT showed comparable free GFP to GFP-CfAtg8 while Δ*Cfrad6* showed higher free GFP than GFP-CfAtg8 (Fig. 4c). Additionally, the autophagic flux was also quantitatively calculated by measuring the GFP relative to GFP + GFP-CfAtg8 ratio. The ratios of Δ*Cfrad6* were both higher than that in WT under CM and MM-N

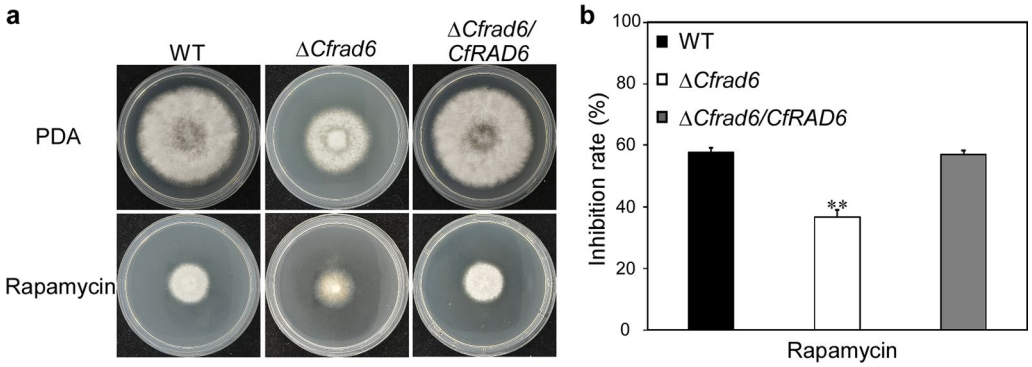

Fig. 3 CfRad6 is involved in the response to rapamycin. **a** The WT, Δ*Cfrad6,* and Δ*Cfrad6/CfRAD6* strains were incubated on PDA plates with 25 nM rapamycin at 28℃ for 3 days. **b** Statistics analysis of growth inhibition rates of the strains to rapamycin stress; Error bars represent the standard deviation (SD) of three replicates, and asterisks indicate the difference is significant ($P < 0.01$)

conditions (Fig. 4c). These results suggest that CfRad6 plays a negative role in autophagy.

We next tested whether CfRad6 plays a direct role in autophagy by interacting with CfAtg8. However, Y2H assays revealed that yeast cells transformed with CfRad6/CfAtg8 did not grow on the SD-Leu-Trp-His and SD-Leu-Trp-His-Ade medium (Additional file 1: Figure S3a), indicating that there was no direct interaction between CfRad6 and CfAtg8. BiFC assays also confirmed that CfRad6 did not interact directly with CfAtg8 in autophagy induction conditions (Additional file 1: Figure S3b).

The studies conducted in *Homo sapiens* showed that proteasome malfunction activates the autophagy pathway (Zheng et al. 2011; Ji and Kwon 2017; Su and Wang 2020). We thus use the 26S proteasome inhibitor MG132 (z-Leu-Leu-Leu-CHO) to verify its roles in the autophagy of *C. fructicola*. Although the treatments with MG132 showed similar autophagosome numbers to those in CM conditions (Fig. 4d,e), the autophagy level of the treatments with MG132 was higher than in CM conditions (Fig. 4f).

CfRad6 is important for growth and conidiation

To investigate whether CfRad6 participates in regulating the vegetative growth of *C. fructicola*, the WT, Δ*Cfrad6,* and Δ*Cfrad6/CfRAD6* strains were cultured on PDA and MM plates for 3 days and measured their colony diameters. The results showed that the colonies of Δ*Cfrad6* on PDA and MM medium were significantly smaller than those of WT and complemented strains (Fig. 5a,b). The results showed that CfRad6 is involved in regulating the vegetative growth of *C. fructicola*.

Conidia are crucial for infecting host cells of *C. fructicola*. To investigate whether CfRad6 affects the conidiation of *C. fructicola*, we quantified the conidia of WT, Δ*Cfrad6*, and Δ*Cfrad6/CfRAD6* that were cultured on a 28°C and 180 rpm shaker for 2 days. The results showed that Δ*Cfrad6* produced significantly fewer conidia than WT and Δ*Cfrad6/CfRAD6* (Fig. 5c). These results indicate that CfRad6 is important for the conidiation of *C. fructicola*.

CfRad6 is required for the full pathogenicity of *C. fructicola*

We are most concerned about the contribution of CfRad6 to the pathogenicity of *C. fructicola*, so we inoculated the WT, Δ*Cfrad6*, and Δ*Cfrad6/CfRAD6* strains on the leaves of wounded and healthy *C. oleifera* leaves. The Δ*Cfrad6* mutant only formed very small disease spots on the wounded leaves but did not develop lesions on the healthy leaves, in contrast to the typical and large lesions produced by the WT and Δ*Cfrad6/CfRAD6* strains (Fig. 6a–d). To further investigate the specificity of CfRad6 in pathogenicity, we also inoculated the above strains on apples and found that the lesions caused by the Δ*Cfrad6* mutant were significantly smaller than those formed by the WT and Δ*Cfrad6/CfRAD6* strains (Fig. 6e,f). These results suggest that CfRad6 is required for the full pathogenicity of *C. fructicola* on its hosts.

CfRad6 mediates the appressoria formation and lipid and glycogen metabolism of *C. fructicola*

Appressoria play a crucial role in the infection of hosts by *Colletotrichum* spp. (Fukada and Kubo 2015; Fukada et al. 2019; Ryder et al. 2022). To investigate the underlying mechanism of the pathogenicity defects of Δ*Cfrad6*, we examined the appressoria formation of WT, Δ*Cfrad6*, and Δ*Cfrad6/CfRAD6* after they were cultured on hydrophobic glass slides for 24 h. The result revealed that Δ*Cfrad6* showed a significant decrease in germination rates for Δ*Cfrad6* compared to WT and Δ*Cfrad6/CfRAD6* (Fig. 7a,b). In addition, we

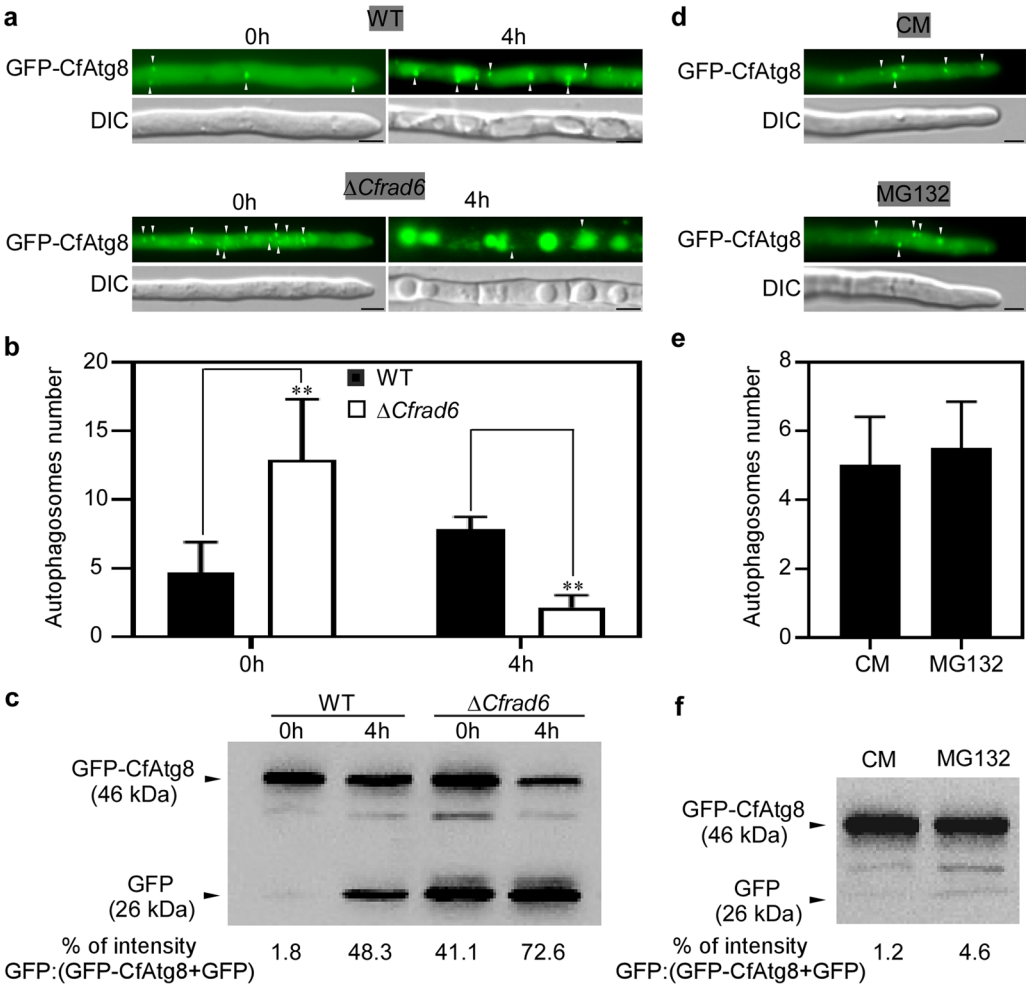

Fig. 4 CfRad6 negatively regulates autophagy. **a** Micrographs of GFP-CfAtg8 labeled autophagosomes in the WT and Δ*Cfrad6* mutant strains. **b** Statistical analysis of autophagosome numbers in the WT and Δ*Cfrad6* mutant strains. On average, more than 50 hyphal tips (about 50 μm in length) were observed. The assays were repeated three times, and the results were similar. **c** Immunoblot analysis of GFP-CfAtg8 proteolysis in the WT and Δ*Cfrad6* mutant. The upper lanes point to the full GFP-Atg8 (46 kDa), and the lower lanes point to the free GFP (26 kDa). The autophagy level was estimated by calculating the amount of free GFP relative to the total amount of full GFP-CfAtg8 plus free GFP. **d** Micrographs of GFP-CfAtg8 labeled autophagosomes in WT with or without MG132 treatment. **e** Statistical analysis of autophagosome numbers in WT with or without MG132 treatment. **f** Immunoblot analysis of GFP-CfAtg8 proteolysis in the WT with or without MG132 treatment

also observed that Δ*Cfrad6* hardly formed appressoria, unlike the more than 70% appressoria formation rate for WT and Δ*Cfrad6/CfRAD6* (Fig. 7a,b). This suggests that CfRad6 mediates the appressoria formation of *C. fructicola*.

The lipids and glycogen in conidia are critical sources of nutrients for appressorium (Wang et al. 2007; Li et al. 2017). We used Nile red to stain lipids and found that lipids began transferring from conidia to appressoria at 8 hpi and almost disappeared at 48 hpi in WT, but lipids were still clearly observed in conidia and germ tubes of Δ*Cfrad6* (Fig. 7c). Similar results were also found in the glycogen staining with KI/I_2 (Additional file 1: Figure S4). This indicates that CfRad6 mediates the lipid and glycogen metabolism of *C. fructicola*.

CfRad6 is involved in response to environmental stresses

The endoplasmic reticulum (ER) is the site of intracellular protein modification, and studies have revealed that pathogens face host-derived ER stress during infection (Tang et al. 2020; Yin et al. 2020). To analyze whether CfRad6 is involved in responding to ER stress, the WT, Δ*Cfrad6*, and Δ*Cfrad6/CfRAD6* strains were cultured on PDA medium with 5.0 mM DTT. The results showed that the inhibition rate of Δ*Cfrad6* was significantly higher than that of WT and Δ*Cfrad6/CfRAD6* (Fig. 8a,b). This

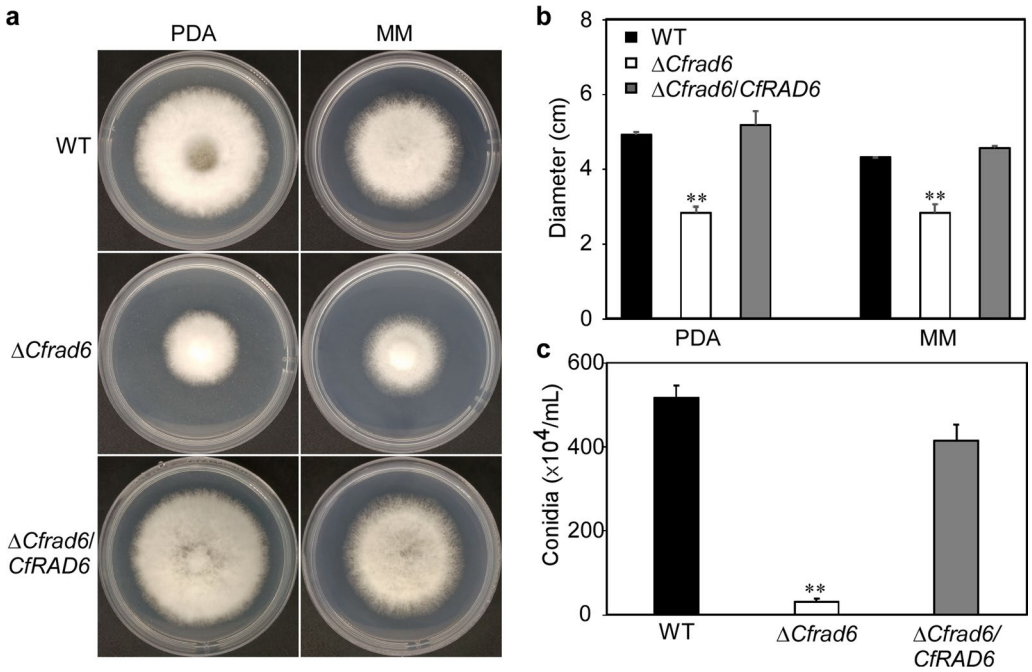

Fig. 5 CfRad6 is important for growth and conidiation. **a** The growth of WT, Δ*Cfrad6,* and Δ*Cfrad6/CfRAD6* strains in PDA and MM medium for 3 days. **b** The diameters of strains were measured and statistically analyzed. Asterisks mean the difference is significant ($P < 0.01$). **c** Statistics analysis of conidia

indicates that CfRad6 mediates the response of *C. fructicola* to ER stress.

The cell wall is the first barrier between the fungi and the environment, acting as a defense against external stress (Levin 2011; Malavazi et al. 2014). To assess whether CfRad6 plays a role in the cell wall integrity stress response, the WT, Δ*Cfrad6*, and Δ*Cfrad6/CfRAD6* strains were cultured on PDA medium with 400 μg/mL CR and 0.1% SDS. The results showed that the Δ*Cfrad6* mutant had a significantly lower inhibition rate on CR than the WT and Δ*Cfrad6*/*CfRAD6* strains and a significantly higher inhibition rate on SDS (Fig. 8c,d). Additionally, we observed that the Δ*Cfrad6* mutant are more sensitive to osmotic stress (Fig. 8e,f). These findings indicate that CfRad6 plays a role in responding to cell wall integrity stress and osmotic stress.

Discussion

In the present study, we identified an E2 protein Rad6 in *C. fructicola*, and found that CfRad6 interacts with three E3 proteins to regulate the growth, conidiation, appressoria formation, stress responses, autophagy, and pathogenicity of *C. fructicola*.

Similar to the homologs of Rad6 proteins in *S. cerevisiae* and *M. oryzae*, CfRad6 contains a ubiquitin-coupled catalysis (UBCc) domain (Shi et al. 2016). By combining the conserved UBCc domain with phylogenetic analysis, we concluded that there is a sequence similarity among Rad6 proteins. Additionally, we found that CfRad6 directly interacts with CfRad18, CfUbr1, and CfBre1, which is consistent with the facts that Rad6 functions in conjunction with three E3 proteins in yeast and the rice blast fungus (Enserink and Kolodner 2012; Shi et al. 2016). Therefore, we proposed that there is also functional similarity among Rad6 proteins.

As expected, the deletion of *CfRAD6* caused a decrease in the growth rate, which is consistent with the positive roles on growth of its homologs in *Caenorhabditis elegans* and *S. cerevisiae* (Enserink and Kolodner 2012; Skibinski and Boyd 2012). Additionally, the Δ*Cfrad6* mutant also showed a similar reduction in conidial production to the *RAD6*-deleted strain in *M. oryzae* (Shi et al. 2016). Together, these results suggest that Rad6 proteins not only share similarity in amino acid sequence but also have conserved functions in growth and conidiation.

Our findings suggest that CfRad6 is involved in response to autophagy inducer rapamycin, indicating its involvement in autophagy, which is further corroborated by the increased autophagosome abundance in the Δ*Cfrad6* mutant. Moreover, the immunoblot analysis also revealed a higher autophagy level in the Δ*Cfrad6* mutant. Thus, we hypothesized that the abnormal UPS could activate the autophagy pathway, which is in line with studies showing that proteasome inhibition or

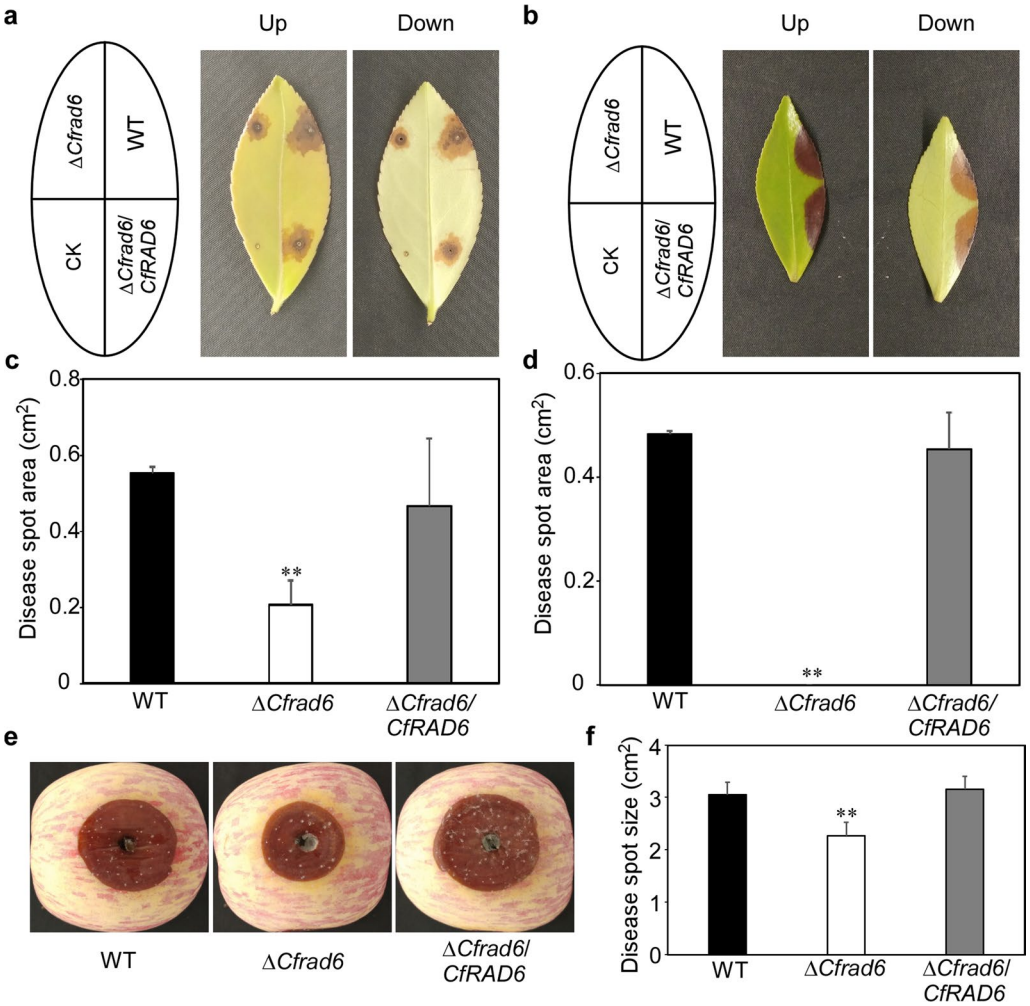

Fig. 6 CfRad6 is required for full pathogenicity. **a** The WT, Δ*Cfrad6*, Δ*Cfrad6/CfRAD6* strains were inoculated on wounded *C. oleifera* leaves. **b** The WT, Δ*Cfrad6*, Δ*Cfrad6/CfRAD6* strains were inoculated on healthy *C. oleifera* leaves. **c** The disease spot areas of strains on wounded *C. oleifera* leaves were measured by ImageJ and statistically analyzed. **d** The disease spot areas of strains on healthy *C. oleifera* leaves were measured by ImageJ and statistically analyzed. **e** The strains were inoculated on wounded apples and photographed. **f** Statistical analysis of disease spots on apples. CK: compared control. Asterisks indicate the difference is significant ($P < 0.01$)

proteasome functional insufficiency can activate compensatory autophagy in *Homo sapiens* (Cha-Molstad et al. 2015; Wang and Wang 2015; Bao et al. 2017). However, CfRad6 did not directly interact with CfAtg8. Further studies are warranted to illustrate how the ubiquitin system links autophagy. A recent study in *M. oryzae* has shown that Ubp3-mediated de-ubiquitination regulates ribophagy but not autophagy (Cai et al. 2022). Nonetheless, we have demonstrated the crosstalk between UPS and autophagy in phytopathogenic fungi for the first time. Recently, we revealed the essential roles of autophagy in the pathogenicity of *C. fructicola* (Guo et al. 2022; Zhang et al. 2022). The disordered autophagy flux might foretell its defects in pathogenicity.

We have found that Δ*Cfrad6* is non-pathogenic on the healthy leaves of *C. oleifera* and shows decreased pathogenicity on the wounded leaves of *C. oleifera* or apples. We reason that the pathogenicity defects of Δ*Cfrad6* are directly caused by the decreased appressoria formation rate. Furthermore, the irregular response to environmental stresses of Δ*Cfrad6*, especially the ER stress, which is likewise derived from the host under pathogenic fungi infection (Tang et al. 2020; Yin et al. 2020), may also be a reason for the pathogenicity defect of Δ*Cfrad6*. Intriguingly, the non-pathogenicity caused by Δ*Cfrad6* on healthy leaves showed a slight difference with the study in *M. oryzae*, which revealed that the *MoRAD6* gene deletion

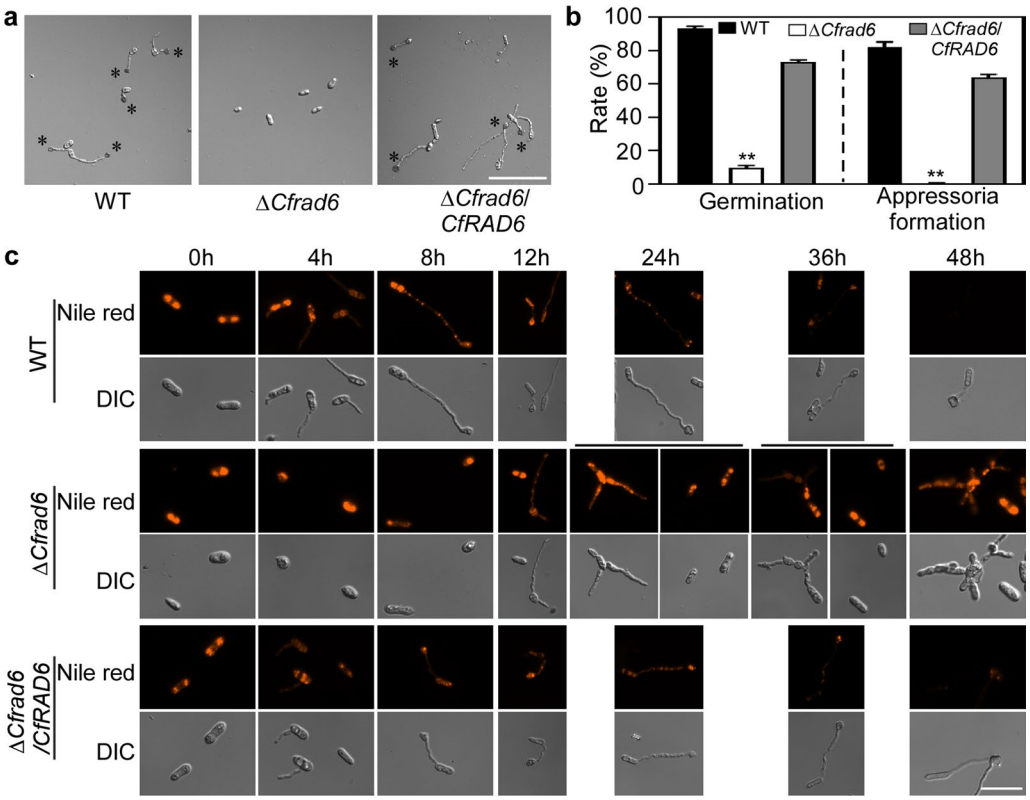

Fig. 7 CfRad6 mediates the appressoria formation and lipid transfer. **a** The conidia of WT, Δ*Cfrad6*, Δ*Cfrad6/CfRAD6* strains were cultured on hydrophobic glasses for 48 h, and appressoria formation were observed. **b** Statistical analysis of appressoria formation rates. Asterisks indicate the difference is significant ($P < 0.01$). Bar = 40 μm. **c** Lipids in conidia and appressoria of the WT, Δ*Cfrad6*, and Δ*Cfrad6/CfRAD6* strains were stained with Nile red at different time points. Bar = 20 μm

mutant still formed disease symptoms (Shi et al. 2016). This slight contradiction also occurred in our previous studies on CfGcn5. We found that the *CfGCN5* gene deletion mutant showed non-pathogenicity on healthy *C. oleifera* leaves (Zhang et al. 2021, 2022), whereas the deletion strain in *M. oryzae* still showed lesions on the host, although the lesions were decreased compared to WT (Zhang et al. 2017). Therefore, we presume that it may be because the epidermis of *C. oleifera* leaves is thicker than that of rice leaves, resulting in Δ*Cfrad6* failing to infect *C. oleifera* leaves, but further studies are highly warranted.

Conclusions

Our study revealed that CfRad6 shows pleiotropic functions in *C. fructicola*, playing an important role in growth, conidiation, appressoria formation, stress response, autophagy and pathogenicity of *C. fructicola*. Therefore, CfRad6 can be considered as a potential target for fungicide development to control anthracnose.

Methods

Strains and culture conditions

The strain that was used as wild-type (WT) for transformation in this study was CFLH16. The WT, Δ*Cfrad6*, and Δ*Cfrad6/CfRAD6* strains were cultured on PDA or MM plates at 28℃. The liquid PDB was used to prepare mycelia for DNA extraction. The liquid CM was used to prepare mycelia for protein extraction.

Phylogenetic tree construction and domain prediction

The E2 CfRad6 protein in *C. fructicola* was identified using the known ScRad6 amino acid sequence in yeast as a bait, and its homologous sequences in *C. gloeosporioides*, *F. graminearum*, *M. oryzae*, *A. oryzae*, *A. nidulans*, and *S. cerevisiae* were obtained from NCBI database (https://www.ncbi.nlm.nih.gov/) and constructed the phylogenetic tree by Mega 11.0 program with the Neighbor-joining method. The domain prediction of CfRad6 was performed by SMART website (http://smart.embl-heidelberg.de/).

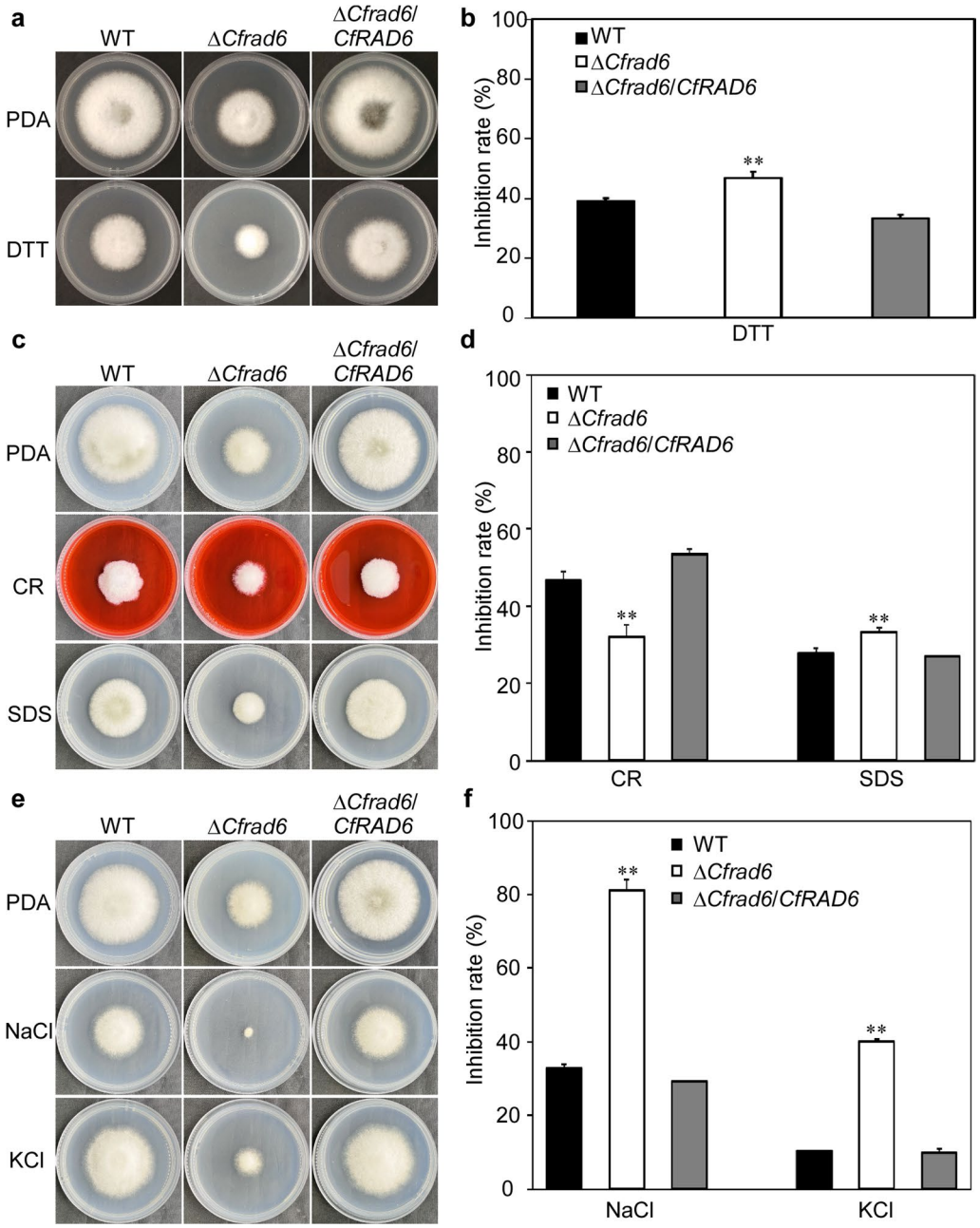

Fig. 8 CfRad6 is involved in responses to environmental stress. **a** The WT, Δ*Cfrad6*, and Δ*Cfrad6/CfRAD6* strains were inoculated in PDA, and PDA supplemented with 5.0 mM DTT for 3 days. **b** Statistical analysis of inhibition rates of the strains to endoplasmic reticulum stress against untreated control. **c** The WT, Δ*Cfrad6*, and Δ*Cfrad6/CfRAD6* strains were inoculated in PDA and PDA plus with 400 μg/mL CR and 0.1% SDS for 3 days. **d** Statistical analysis of inhibition rates of the strains to cell wall integrity stress against untreated control. **e** The WT, Δ*Cfrad6*, and Δ*Cfrad6/CfRAD6* strains were inoculated in PDA and PDA plus with 0.7 M NaCl and 0.6 M KCl for 3 days. **f** Statistical analysis of inhibition rates of the strains to osmotic stress against untreated control. Error bars represent the SD of three replicates, and asterisks indicate the difference is significant ($P < 0.01$)

Gene deletion and complementation

The *CfRAD6* gene deletion was performed using the standard one-step strategy (Zhang et al. 2019, 2021; Li et al. 2021). First, we overlapped the two ~ 1.0 kb sequences flanking *CfRAD6* to the two sides of the *HPH* gene (~ 1.0 kb). Then, we amplified and transformed the ~ 3.4 kb fragments containing the flanking sequences and hygromycin resistance cassette into protoplasts of WT. Finally, the complement fragments were amplified by PCR with primers (Additional file 2: Table S1) and

inserted into pYF11 (bleomycin resistance) to complement the mutant strain.

RT-qPCR analysis

Total RNA was extracted from WT, Δ*Cfrad6*, and Δ*Cfrad6/CfRAD6* strains cultured on liquid CM for 36 h, and then the total RNA was quality controlled and transcribed to cDNA. The RT-qPCR with primers (Additional file 2: Table S1) was run on an ABI QuantStudio 3, and the relative quantification of transcription was normalized to the stable expression *ACTIN* gene. The experiment was repeated three times, and each experiment used independent biological replicates.

Growth, conidiation and appressoria formation assays

The strains of WT, Δ*Cfrad6*, and Δ*Cfrad6/CfRAD6* were cultured on PDA and MM plates for 3 days, then the colony diameters were measured and statistically analyzed. All experiments were repeated three times, each with three replicates. For conidia production assays, mycelia were grown on liquid PDB in an incubation shaker for 48 h, then were filtered with three layers of lens paper, and conidia were collected and quantified. For appressoria formation assays, droplets of conidial suspension were dripped on hydrophobic glasses and incubated at 28°C for 24 h, followed by observation under the microscope (ZEISS, Axio Observer. A1).

Nile red and glycogen staining

For glycogen staining, the conidia of WT, Δ*Cfrad6*, and Δ*Cfrad6/CfRAD6* strains were incubated on hydrophobic glasses for different time points and stained with a solution consisting of 120 mg/mL of KI and 20 mg/mL of I2 in distilled water for 30 min. Yellowish brown deposits can be observed in the bright field immediately. For lipid bodies staining, samples above were stained with Nile red (N8440 Solarbio) to detect neutral lipids for 5 min, then orange-red was visible under a fluorescent microscope. The Nile red was used at 10 μg/mL (stock 1 mg/mL in ethanol) in PBS buffer. All samples were examined and photographed with the fluorescent microscope (ZEISS, Axio Observer. A1).

Stresses response analysis

The WT, Δ*Cfrad6*, and Δ*Cfrad6/CfRAD6* strains were cultured on PDA, and PDA supplemented with 25 nM rapamycin, endoplasmic reticulum stress (5.0 mM DTT), cell wall integrity stress (0.1% SDS, 400 μg/mL CR) and osmotic stress (0.7 M NaCl, 0.6 M KCl) for 3 days, then the colony diameters were measured, and the inhibition rates were statistically analyzed.

Pathogenicity assays

The WT, Δ*Cfrad6*, and Δ*Cfrad6/CfRAD6* strains were inoculated onto the edge of wounded and healthy tea-oil leaves, moisturizing culture in an incubator for 2 days, then its lesions were observed, photographed and analyzed. For the pathogenicity on wounded apples, the apples were first punched into several 4-mm-diameter holes, then the same strains were inoculated onto it. The apples were cultured for 4–5 days, and then the lesions were observed and photographed.

Yeast two-hybrid and BiFC assays

The yeast two-hybrid assay was performed according to the instructions of Alkali-Cation ™ Yeast Transformation Kit. The coding sequences of each candidate gene were amplified with primers listed in Table S1 from cDNA library of WT, inserted into the bait vector pGBKT7 digested by BamHI and prey vector pGADT7 digested by BamHI, respectively, and then ligated to the linearized plasmid vector using the one-step ligase of Novozymes, and the plasmid was extracted in *E. coli*. After the sequencing, pairs of plasmids were co-transformed into the yeast strain AH109 and then cultured on SD-Leu-Trp medium. After growing colonies, it was transferred on SD-Leu-Trp-Ade-His medium. The positive control is ADRECT + BD (+), and the negative control is ADRECT + BD (-).

For the BiFC assays, the pHZ68-CfAtg8 and pHZ65-CfRad6 vectors were constructed and used to co-transform the WT strains. The WT strains co-expressing pHZ68-CfAtg8 and pHZ65-CfRad6 were cultured in liquid CM medium for 36 h and washed with sterile water, followed by incubation in MM-N for 4 h and 8 h. The fluorescent signals of the hypha were observed under the fluorescent microscope.

Autophagy induction assays

The WT and Δ*Cfrad6* strains that expressed the GFP-Cf*ATG8* gene were cultured on liquid CM medium for 36 h, and mycelium pellets of that were washed with sterile water, followed by incubated in liquid MM-N or liquid CM plus with 50 μM MG132 for 4 h. The autophagosomes and GFP signals of the hypha were observed under the fluorescent microscope and analyzed.

Western blot analysis

The proteins were exacted from the above-treated mycelium pellets according to our previous method (Zhang et al. 2022), then proteins were analyzed by western blotting with the primary antibodies anti-GFP (rabbit, 1:5,000, Abways, AB0045) or anti-ubiquitin (rabbit, 1:1,000, Zenbio, R26024), and the secondary antibodies

HRP-labeled goat anti-rabbit lgG (H1L) (1:10,000, Abways, AB0101). Finally, an Omni-ECL Femto Light Chemiluminescence Kit (EpiZyme, SQ201) was used to detect the proteins, and the gray analysis was carried out with ImageJ software.

Statistical analysis

All statistical data were performed using a one-way ANOVA (Analysis of Variance) with Duncan's new multiple range test.

Abbreviations

UPS	Ubiquitin–proteasome system
UBCc	Ubiquitin-coupled catalysis
HPH	Hygromycin resistance cassette
WT	Wild type
Y2H	Yeast two-hybrid
CM	Complete medium
MM	Minimal medium
MM-N	Minimal medium lacking N
PDA	Potato dextrose agar
PDB	Potato dextrose broth
PCR	Polymerase chain reaction
RT-PCR	Reverse transcription polymerase chain reaction
RT-qPCR	Reverse transcription quantitative polymerase chain reaction
ER	Endoplasmic reticulum
H_2O_2	Hydrogen peroxide
CR	Congo red
DTT	Dithiothreitol
BIFC	Bimolecular fluorescence complementation

Supplementary Information

The online version contains supplementary material available at https://doi.org/10.1186/s42483-023-00191-z.

Additional file 1: **Figure S1**. Generation of the *CfRAD6* gene deletion mutant in *C. fructicola*. **a** The schematic diagram of *CfRAD6* gene deletion strategy. **b** Identification of *CfRAD6* gene deletion mutant by PCR amplified with primers 1 (35BWF/35HPHR) and primers 2 (35NBF/35NBR). **c** Transcription level of WT, Δ*Cfrad6*, and Δ*Cfrad6/CfRAD6*. **d** Identification of *CfRAD6* gene deletion mutant by RT-PCR amplified with primers 3 (Rad6ADF/Rad6ADR) and primers 4 (actin QF/actin QR). M1: DL 5000 DNA marker; M2: DL 2000 DNA marker; Δ: Mutant; C: Complemented strain; +: Positive control; -: Negative control.**Figure S2**. CfRad6 is not involved in the total protein ubiquitination level.The ubiquitination levels of WT, Δ*Cfrad6* and Δ*Cfrad6/CfRAD6* strains were analyzed by Western blotting with an anti-ubiquitin antibody.**Figure S3**. CfRad6 does not interact with CfAtg8. **a** The co-expressed strains were plated on compared SD-Leu-Trp and selective SD-Leu-Trp-His or SD-Leu-Trp-His-Ade. **b** Micrographs of the co-expressed strains under MM-N induced conditions at 0, 4, and 8 h. Bars = 5 μm.**Figure S4**. CfRad6 regulates the utilization of glycogen. Glycogen in conidia and appressoria of the WT, Δ*Cfrad6*, and Δ*Cfrad6/CfRAD6* strains was stained with KI/I2 at different time points. Bar = 20 μm.

Additional file 2: Table S1. Primers used in this study.

Acknowledgements

Not applicable.

Author contributions

HL and SZ conceived and designed the study. JL, YG, YC, and SZ performed the experiments. JL and SZ wrote the manuscript. All authors read and approved the final manuscript.

Funding

This research was funded by the National Natural Science Foundation of China (32001317).

Availability of data and materials

Not applicable.

Declarations

Ethics approval and consent to participate

Not applicable.

Consent for publication

Not applicable.

Competing interests

The authors declare that they have no competing interests.

Received: 22 February 2023 Accepted: 26 July 2023
Published online: 28 August 2023

References

Bao X, Ren T, Huang Y, Ren C, Yang K, Zhang H, et al. Bortezomib induces apoptosis and suppresses cell growth and metastasis by inactivation of Stat3 signaling in chondrosarcoma. Int J Oncol. 2017;50:477–86. https://doi.org/10.3892/ijo.2016.3806.

Cai X, Xiang S, He W, Tang M, Zhang S, Chen D, et al. Deubiquitinase Ubp3 regulates ribophagy and deubiquitinates Smo1 for appressorium-mediated infection by *Magnaporthe oryzae*. Mol Plant Pathol. 2022;23:832–44. https://doi.org/10.1111/mpp.13196.

Cha-Molstad H, Sung KS, Hwang J, Kim KA, Yu JE, Yoo YD, et al. Amino-terminal arginylation targets endoplasmic reticulum chaperone BiP for autophagy through p62 binding. Nat Cell Biol. 2015;17:917–29. https://doi.org/10.1038/ncb3177.

Ciechanover A. Proteolysis: from the lysosome to ubiquitin and the proteasome. Nat Rev Mol Cell Biol. 2005;6:79–87. https://doi.org/10.1038/nrm1552.

Enserink JM, Kolodner RD. What makes the engine hum: Rad6, a cell cycle supercharger. Cell Cycle. 2012;11:249–52. https://doi.org/10.4161/cc.11.2.19023.

Fukada F, Kubo Y. *Colletotrichum orbiculare* regulates cell cycle G1/S progression via a two-component GAP and a GTPase to establish plant infection. Plant Cell. 2015;27:2530–44. https://doi.org/10.1105/tpc.15.00179.

Fukada F, Kodama S, Nishiuchi T, Kajikawa N, Kubo Y. Plant pathogenic fungi *Colletotrichum* and *Magnaporthe* share a common G(1) phase monitoring strategy for proper appressorium development. New Phytol. 2019;222:1909–23. https://doi.org/10.1111/nph.15728.

Guo Y, Chen Z, Li H, Zhang S. The CfSnt2-dependent deacetylation of histone H3 mediates autophagy and pathogenicity of *Colletotrichum fructicola*. J Fungi (basel). 2022. https://doi.org/10.3390/jof8090974.

Imura Y, Molho M, Chuang C, Nagy PD. Cellular Ubc2/Rad6 E2 ubiquitin-conjugating enzyme facilitates tombusvirus replication in yeast and plants. Virology. 2015;484:265–75. https://doi.org/10.1016/j.virol.2015.05.022.

Jentsch S, McGrath JP, Varshavsky A. The yeast DNA repair gene *RAD6* encodes a ubiquitin-conjugating enzyme. Nature. 1987;329:131–4. https://doi.org/10.1038/329131a0.

Ji CH, Kwon YT. Crosstalk and interplay between the ubiquitin-proteasome system and autophagy. Mol Cells. 2017;40:441–9. https://doi.org/10.14348/molcells.2017.0115.

Jia W, Liu G, Zhang P, Li H, Peng Z, Wang Y, et al. The ubiquitin-26S proteasome pathway and its role in the ripening of fleshy fruits. Int J Mol Sci. 2023. https://doi.org/10.3390/ijms24032750.

Jiang SQ, Li H. First report of leaf anthracnose caused by *Colletotrichum karstii* on tea-oil trees (*Camellia oleifera*) in China. Plant Dis. 2018. https://doi.org/10.1094/PDIS-08-17-1195-PDN.

Levin DE. Regulation of cell wall biogenesis in *Saccharomyces cerevisiae*: the cell wall integrity signaling pathway. Genetics. 2011;189:1145–75. https://doi.org/10.1534/genetics.111.128264.
Li H, Zhou GY, Liu JA, Xu J. Population genetic analyses of the fungal pathogen *Colletotrichum fructicola* on tea-oil Trees in China. PLoS ONE. 2016;11:e0156841. https://doi.org/10.1371/journal.pone.0156841.
Li X, Gao C, Li L, Liu M, Yin Z, Zhang H, et al. MoEnd3 regulates appressorium formation and virulence through mediating endocytosis in rice blast fungus Magnaporthe oryzae. PLoS Pathog. 2017;13:e1006449. https://doi.org/10.1371/journal.ppat.1006449.
Li S, Zhang S, Li B, Li H. The SNARE protein CfVam7 is required for growth, endoplasmic reticulum stress response, and pathogenicity of *Colletotrichum fructicola*. Front Microbiol. 2021;12:736066. https://doi.org/10.3389/fmicb.2021.736066.
Ma T, Zhang L, Wang M, Li Y, Jian Y, Wu L, et al. Plant defense compound triggers mycotoxin synthesis by regulating H2B ub1 and H3K4 me2/3 deposition. New Phytol. 2021;232:2106–23. https://doi.org/10.1111/nph.17718.
Malavazi I, Goldman GH, Brown NA. The importance of connections between the cell wall integrity pathway and the unfolded protein response in filamentous fungi. Brief Funct Genom. 2014;13:456–70. https://doi.org/10.1093/bfgp/elu027.
Marroquin-Guzman M, Wilson RA. GATA-dependent glutaminolysis drives appressorium formation in *Magnaporthe oryzae* by suppressing TOR inhibition of cAMP/PKA signaling. PLoS Pathog. 2015;11:e1004851. https://doi.org/10.1371/journal.ppat.1004851.
Mizushima N, Komatsu M. Autophagy: renovation of cells and tissues. Cell. 2011;147:728–41. https://doi.org/10.1016/j.cell.2011.10.026.
Mukhopadhyay D, Riezman H. Proteasome-independent functions of ubiquitin in endocytosis and signaling. Science. 2007;315:201–5. https://doi.org/10.1126/science.1127085.
Ohsumi Y. Historical landmarks of autophagy research. Cell Res. 2014;24:9–23. https://doi.org/10.1038/cr.2013.169.
Pohl C, Dikic I. Cellular quality control by the ubiquitin-proteasome system and autophagy. Science. 2019;366:818–22. https://doi.org/10.1126/science.aax3769.
Ridenour JB, Smith JE, Hirsch RL, Horevaj P, Kim H, Sharma S, et al. UBL1 of *Fusarium verticillioides* links the N-end rule pathway to extracellular sensing and plant pathogenesis. Environ Microbiol. 2014;16:2004–22. https://doi.org/10.1111/1462-2920.12333.
Ryder LS, Cruz-Mireles N, Molinari C, Eisermann I, Eseola AB, Talbot NJ. The appressorium at a glance. J Cell Sci. 2022;135:jcs259857. https://doi.org/10.1242/jcs.259857.
Shi HB, Chen GQ, Chen YP, Dong B, Lu JP, Liu XH, et al. MoRad6-mediated ubiquitination pathways are essential for development and pathogenicity in *Magnaporthe oryzae*. Environ Microbiol. 2016;18:4170–87. https://doi.org/10.1111/1462-2920.13515.
Shukla PK, Sinha D, Leng AM, Bissell JE, Thatipamula S, Ganguly R, et al. Mutations of Rad6 E2 ubiquitin-conjugating enzymes at alanine-126 in helix-3 affect ubiquitination activity and decrease enzyme stability. J Biol Chem. 2022;298:102524. https://doi.org/10.1016/j.jbc.2022.102524.
Skibinski GA, Boyd L. Ubiquitination is involved in secondary growth, not initial formation of polyglutamine protein aggregates in *C. elegans*. BMC Cell Biol. 2012;13:10–10. https://doi.org/10.1186/1471-2121-13-10.
Stewart MD, Ritterhoff T, Klevit RE, Brzovic PS. E2 enzymes: more than just middle men. Cell Res. 2016;26:423–40. https://doi.org/10.1038/cr.2016.35.
Su H, Wang X. Proteasome malfunction activates the PPP3/calcineurin-TFEB-SQSTM1/p62 pathway to induce macroautophagy in the heart. Autophagy. 2020;16:2114–6. https://doi.org/10.1080/15548627.2020.1816666.
Tang W, Jiang H, Aron O, Wang M, Wang X, Chen J, et al. Endoplasmic reticulum-associated degradation mediated by MoHrd1 and MoDer1 is pivotal for appressorium development and pathogenicity of *Magnaporthe oryzae*. Environ Microbiol. 2020;22:4953–73. https://doi.org/10.1111/1462-2920.15069.
Ulrich HD, Walden H. Ubiquitin signalling in DNA replication and repair. Nat Rev Mol Cell Biol. 2010;11:479–89. https://doi.org/10.1038/nrm2921.
Wang C, Wang X. The interplay between autophagy and the ubiquitin-proteasome system in cardiac proteotoxicity. Biochim Biophys Acta. 2015;1852:188–94. https://doi.org/10.1016/j.bbadis.2014.07.028.
Wang ZY, Soanes DM, Kershaw MJ, Talbot NJ. Functional analysis of lipid metabolism in Magnaporthe grisea reveals a requirement for peroxisomal fatty acid beta-oxidation during appressorium-mediated plant infection. Mol Plant Microbe Interact. 2007;20:475–91. https://doi.org/10.1094/mpmi-20-5-0475.
Wu L, Li J, Li Z, Zhang F, Tan X. Transcriptomic analyses of *Camellia oleifera* "Huaxin" leaf reveal candidate genes related to long-term cold stress. Int J Mol Sci. 2020. https://doi.org/10.3390/ijms21030846.
Yamamoto T, Mori Y, Ishibashi T, Uchiyama Y, Sakaguchi N, Furukawa T, et al. Characterization of Rad6 from a higher plant, rice (*Oryza sativa* L.) and its interaction with Sgt1, a subunit of the SCF ubiquitin ligase complex. Biochem Biophys Res Commun. 2004;314:434–9. https://doi.org/10.1016/j.bbrc.2003.12.144.
Yin Z, Feng W, Chen C, Xu J, Li Y, Yang L, et al. Shedding light on autophagy coordinating with cell wall integrity signaling to govern pathogenicity of *Magnaporthe oryzae*. Autophagy. 2020;16:900–16. https://doi.org/10.1080/15548627.2019.1644075.
Zhang S, Liang M, Naqvi NI, Lin C, Qian W, Zhang LH, et al. Phototrophy and starvation-based induction of autophagy upon removal of Gcn5-catalyzed acetylation of Atg7 in *Magnaporthe oryzae*. Autophagy. 2017;13:1318–30. https://doi.org/10.1080/15548627.2017.1327103.
Zhang C, Song L, Choudhary MK, Zhou B, Sun G, Broderick K, et al. Genome-wide analysis of genes encoding core components of the ubiquitin system in soybean (Glycine max) reveals a potential role for ubiquitination in host immunity against soybean cyst nematode. BMC Plant Biol. 2018;18:149. https://doi.org/10.1186/s12870-018-1365-7.
Zhang S, Guo Y, Li S, Zhou G, Liu J, Xu J, et al. Functional analysis of CfSnf1 in the development and pathogenicity of anthracnose fungus *Colletotrichum fructicola* on tea-oil tree. BMC Genet. 2019;20:94. https://doi.org/10.1186/s12863-019-0796-y.
Zhang S, Guo Y, Chen S, Li H. The Histone acetyltransferase CfGcn5 regulates growth, development, and pathogenicity in the anthracnose fungus *Colletotrichum fructicola* on the tea-oil tree. Front Microbiol. 2021;12:680415. https://doi.org/10.3389/fmicb.2021.680415.
Zhang S, Guo Y, Li S, Li H. Histone acetyltransferase CfGcn5-mediated autophagy governs the pathogenicity of *Colletotrichum fructicola*. Mbio. 2022;13:e0195622. https://doi.org/10.1128/mbio.01956-22.
Zheng Q, Su H, Tian Z, Wang X. Proteasome malfunction activates macroautophagy in the heart. Am J Cardiovasc Dis. 2011;1:214–26. https://doi.org/10.1080/15548627.2020.1816666.
Zhou GA, Chang RZ, Qiu LJ. Overexpression of soybean ubiquitin-conjugating enzyme gene *GmUBC2* confers enhanced drought and salt tolerance through modulating abiotic stress-responsive gene expression in *Arabidopsis*. Plant Mol Biol. 2010;72:357–67. https://doi.org/10.1007/s11103-009-9575-x.